Materials Research. 2017; 20(5): 1166-1173
DOI: http://dx.doi.org/10.1590/1980-5373-MR-2016-0512

Growth and Characterization of $Al_xGa_{1-x}As$ Obtained by Metallic-Arsenic-Based-MOCVD[1]

Roberto Saúl Castillo-Ojeda[a], Joel Díaz-Reyes[b]*, Miguel Galván Arellano[c], María de la Cruz Peralta-Clara[b], Julieta Salomé Veloz-Rendón[b]

[a] *Universidad Politécnica de Pachuca, Carretera Pachuca Cd. Sahagún Km. 20, Rancho Luna, Ex-Hacienda de Sta. Bárbara, Zempoala, Hidalgo, 43830, México*
[b] *Centro de Investigación en Biotecnología Aplicada, Instituto Politécnico Nacional, Ex–Hacienda de San Molino, Km 1.5 de la Carretera Estatal Santa Inés Tecuexcomac-Tepetitla, Tepetitla de Lardizábal, Tlaxcala, 90700, México*
[c] *Departamento de Ingeniería Eléctrica, Sección de Electrónica del Estado Sólido, Centro de Investigación y de Estudios Avanzados, Instituto Politécnico Nacional, Zacatenco, México D. F., 07360, México*

Received: July 8, 2016; Accepted: September 18, 2016

In this work reports results related to growth and characterization of $Al_xGa_{1-x}As$ epilayers, which were grown in a metallic-arsenic-based-MOCVD system. The gallium and aluminium used precursors were trimethylgallium (TMGa) and trimethylaluminium (TMAl), respectively. By photoluminescence measurements observed, that only samples grown at temperatures above 800°C display photoluminescence. Hall measurements on the samples showed highly compensated material. Samples grown at temperatures lower than 750°C were highly resistive. Independently of the V/III ratio; the samples grown at higher temperatures were n-type. As the temperature is increased the layer compensation decreases. The $Al_xGa_{1-x}As$ epilayers resulted n-type with an electron concentration of 1×10^{17} cm^{-3} and a corresponding carrier mobility of ~2200 $cm^2/V\times s$. Raman spectra show vibrational bands associated to TO-GaAs-like (262 cm^{-1}), LO-GaAs-like (275 cm^{-1}), TO-AlAs-like (369 cm^{-1}) and LO-AlAs-like (377 cm^{-1}). The Raman spectra show the epilayers become more defective as the growth temperature is increased. The chemical composition was studied by SIMS exhibit the presence of silicon, carbon and oxygen as main residual impurities. The silicon concentration of ~1.0×10^{17} cm^{-3} is very close to the carrier concentration determined by the van der Pauw measurements. The residual oxygen detected on the samples maybe responsible of the weak photoluminescence signal of the $Al_xGa_{1-x}As$ layers.

Keywords: *Elemental arsenic, MOCVD-$Al_xGa_{1-x}As$/GaAs epilayers, Hall Effect, 12K photoluminescence, Atomic force microscopy surface morphology*

1. Introduction

Among the III-V semiconductor materials, GaAs and $Al_xGa_{1-x}As$ have been widely studied. This is due to their optical and electrical properties. Nowadays is very common to find a large variety of devices based on these materials, lasers for commercial CDs, high mobility transistors, electro-optical switches, are only a few examples of the wide field of applications of these devices made up with $Al_xGa_{1-x}As$/GaAs epitaxial layers. In order to obtain these epitaxial layers with the desired characteristics for the electronic application is necessary to grow them with the adequate degree of purity and crystalline quality. Features as thickness control, suitable electrical and optical properties, crystal quality, are tightly associated with the growth technique used for its preparation. Molecular Bean Epitaxy (MBE), Liquid Phase Epitaxy (LPE) and Metal Organic Chemical Vapour Deposition (MOCVD) are the most successful ones. Nevertheless, each of them has important advantages and disadvantages. The Metal Organic Chemical Vapour Deposition (MOCVD) system has been widely used for the growth of epitaxial semiconductors layers, with high quality and excellent surface morphology. The most serious difficulty on growing $Al_xGa_{1-x}As$ epitaxial layers by Metal Organic Chemical Vapour Deposition (MOCVD) is the incorporation of carbon and oxygen as residual impurities. These impurities in small concentrations in $Al_xGa_{1-x}As$ epitaxial layers have very strong deleterious effect on their optical and electrical characteristics. However, this technique has as a main problem the use of highly toxic gases, as is the case of arsine and phosphine, both of them used as precursors of the elements of the five family. Liquid Phase Epitaxy (LPE) has as main problem the thickness control and surface morphology. The Molecular Beam Epitaxy uses an expensive growth system in reference to the initial investment and the operational costs. As we mentioned before, MOCVD has as a main problem, the use of toxic gases, this disadvantage has been the main

[1] Article presented and selected from "The XXIV International Materials Research Congress (IMRC) 2015". Symposium 5B "Structural and Chemical Characterization of Metals, Alloys and Compounds". Cancun, Mexico August 16-20, 2015.

* e-mail: joel_diaz_reyes@hotmail.com

motor for searching alternative precursor sources for the arsine substitution. The use of MOCVD systems in which the arsine has been substituted by solid arsenic is cheaper and safer. In this work, we present the results obtained using one of these systems MOCVD growth modified, where the arsine has been replaced by elemental arsenic. Solid arsenic is safe to handle, due to its low vapour pressure at room temperature, additionally; the growth reactor is easy to clean with common chemical solutions. However, it is highly recommended to follow the security protocols as to vent adequately the work area and to have the growth system in a closed and efficient vapour extraction hood. Besides, it is necessary to install a burning system in the exhaust of the growth chamber for cracking the byproducts of the process including the possible arsine molecules that could be produce as result of the reaction in the growth processes.

2. Experimental Details

The growth runs were done on both, Si-doped GaAs substrate and semi-insulating (100) oriented Cr-doped GaAs substrates, miss oriented *±4 degree* toward the (110) direction. The substrate preparation involves, as usual, degreasing by organic solvents, surface oxide elimination by HCl and a surface decaping by chemical etching using H_2SO_4:H_2O_2:H_2O (5:1:1). As a last step, the substrates were rinsed in deionized water and dried by nitrogen blowing to eliminate any trace of water. The samples were grown using electronic grade trimethylgallium (TMGa), trimethylaluminium (TMAl), as gallium and aluminium precursors, respectively, and metallic arsenic (9N) as the arsenic source. The solid arsenic is placed in a quartz ampoule with only one open end. The arsenic supply to the growth surface was controlled by a second independent furnace based on an electrical resistance heater. Arsenic flux to the growth surface was only controlled by the temperature of this quartz ampoule. It was not used a carrier gas for the arsenic flux, instead of this, the arsenic was introduced by diffusion on the growth zone by controlling the temperature of the arsenic source. The used MOCVD system consists of a horizontal quartz tube operating at atmospheric pressure. The substrates were placed on a graphite substrate holder and heated by a set of infrared lamps. The V/III ratio in the growth runs can be easily adjusted by controlling the arsenic source temperature or by adjusting the hydrogen flow through the metalorganic vessels, by means of electronic mass flow controllers (MFC). In most experiments, this V/III ratio was ~50. The growth atmosphere was provided using a palladium-silver alloy hydrogen purifier. The main characteristics and details of the MOCVD reactor used for growing the samples have been published elsewhere[1,2]. After the substrate preparation, the first grown layer was a GaAs buffer layer, the thickness of this buffer layer was approximately 0.2 μm and in some cases 0.5 μm. The $Al_xGa_{1-x}As$ layers studied in this work were grown in a MOCVD growth system of this type, that is modified.

The electrical properties of the layers were studied using Hall effect by Van der Pauw method at 77 and 300 K. The investigated samples were square shaped samples with dimensions of 5.0×5.0 mm^2. The samples were provided with four ohmic contacts by alloying indium small balls on theirs corners, for alloying the contacts on the sample surface; these were annealed at 400°C approximately 1 min in a nitrogen flux. The linearity and symmetry of the ohmic contacts were tested following the procedure described in the ASTM standards[3].

The optical and structural characterizations of layers were performed by 12K photoluminescence and Raman spectroscopy. Photoluminescence measurements of the GaAs buffer and $Al_xGa_{1-x}As$ layers were obtained using the 632.8 nm line of Helium-Neon laser as an excitation source at 20 mW of power. The radiative emission was analysed through a SPEX double monochromator. The samples were mounted in a closed-cycle Helium cryostat at 12 K, special care was taken in order to not produce stress on samples. Assignation of each transition was accomplished studying the behaviour of the PL spectra at different excitation powers. The energy positions and the linewidth at half-maximum (FWHM) of each peak have been determined by multi-Gaussians deconvolution of the PL spectra. Raman scattering experiments were performed at room temperature using the 6328 Å line of a He-Ne laser at normal incidence for excitation. The light was focused to a diameter of 6 μm at the sample using a 50× (numerical aperture 0.9) microscope objective. The nominal laser power used in these measurements was 20 mW. Care was taken to avoid the heating of the sample inadvertently to the point of changing its Raman spectrum. Scattered light was analysed using a micro-Raman system (Lambram model of Dilor), a holographic notch filter made by Kaiser Optical System, Inc. (model superNotch-Plus), a 256×1024-pixel CCD used as detector cooled to 140 K using liquid nitrogen, and two interchangeable gratings (600 and 1800 g/mm). Typical spectrum acquisition time was limited to 60 s to minimize the sample heating effects discussed above. Absolute spectral feature position calibration to better than 0.5 cm^{-1} was performed using the observed position of Si which is shifted by 521.2 cm^{-1} from the excitation line. The chemical composition of the $Al_xGa_{1-x}As$ layers was studied using secondary ion mass spectroscopy. The analytical parameters for these measurements were Cs^+ as primary ions and 10 nA as primary current, the beam diameter was 40 μm with an impact energy of 3 KeV, the bombarded area was 150 μm^2 and the mass resolution (M/ΔM) was 300.

3. Experimental Results and Discussion

3.1. GaAs buffer layer

The substrate temperatures used for growing the GaAs buffer layer were ranged from 600 to 875°C in these cases; the arsenic flux was 7.0 μmol/min and a V/III ratio of ~50.

This arsenic flux corresponds to heat the arsenic ampoule at 560°C in our growth system, in this range, the carrier concentration measured in the grown layers increases as the growth temperature is increased. At 650°C, the electron concentration was approximately 7×10^{15} cm^{-3}, while for samples grown at ~870°C, the electron concentration was approximately 2×10^{17} cm^{-3}. The 300 K carrier mobility of these layers was around μ_n= 2000 $cm^2/V\times s$. It was noted some insensitivity with respect to arsenic temperature. Comparing our results with those of ref.[4], we can estimate that the degree of compensation of the grown samples is higher than 0.6. Additionally, the high degree of compensation of the layers can explain the low mobility presented of these samples. GaAs mobility of samples grown with traditional MOCVD systems using arsine and TMGa are typically higher than 8,000 $cm^2/V\times s$.

3.2. Surface morphology of the buffer layer

The buffer layer surface morphology was evaluated using Atomic Force Microscopy. All the GaAs buffer layers examined, presented an aspect like a mirror surface. In Figure 1 is shown the typical surface aspect of the buffer layer. As can be seen, the roughness of this layer is not larger than 20 nm. The growth temperature of the shown sample was 750°C. Even the elongated structures that appear in these atomic force images can be attributed to the jump of the cantilever produced by adhesive forces during the measurement. The AFM images presented in Figure 1 show a low degree of roughness of the GaAs samples. 10 nm can be considered low for the observation of quantum effects of electron confinement in layered structures.

3.3. 12K photoluminescence of the buffer layer

A typical 12 K photoluminescence spectrum is showed in Figure 2. The photoluminescence peaks identification, in

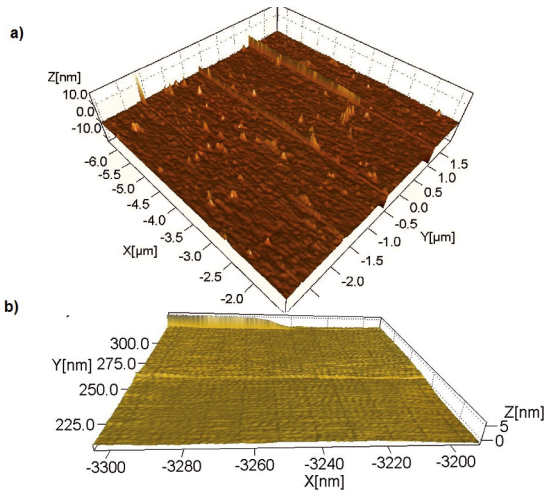

Figure 1: GaAs Buffer Layer Atomic Force Microscopy scan.

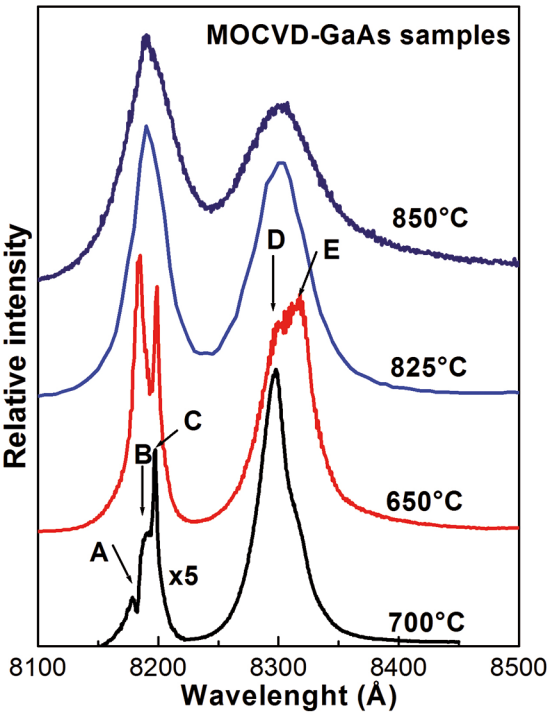

Figure 2: Photoluminescence spectra of the GaAs buffer layers grown at different substrate temperatures.

this emission spectrum, are as follow: The peak labelled as A observed at 8183 Å corresponds to a free exciton recombination, (F,X); The peaks B observed at 8186.7-8187.9 Å correspond to excited state bound to neutral donors, $(D°,X)_{exc}$. The peak C at 8197 Å is associated to J=1/2 exciton bound to neutral acceptor, $(A°,X)_{1=2}$. The peaks labelled as D and E correspond to conduction band to neutral acceptor at 8301 Å, (e-A°), and neutral donor to neutral acceptor at 8325 Å, (D°-A°) transitions[4], both of them associated with carbon as acceptor impurity. The existence of the free exciton peak at 8183 Å, labelled as A, is associated with the good crystalline quality of the GaAs epitaxial layers[5].

3.4. $Al_xGa_{1-x}As$ epitaxial layers

The growth of the ternary semiconductor alloys epitaxial layers presents more difficulties in comparison with the binary semiconductor compound. The electrical properties of these layers were studied using Hall Effect by the Van der Paw method at 77 and 300 K. The results obtained from these measurements are summarized in Table 1. In this Table, as can be seen, the carrier mobility of these samples was around 2000 $cm^2/V\times s$, while the concentration was in the order of 10^{17} cm^{-3}. In some cases, it was not possible to measure the 77K carrier mobility due to the inability of obtaining ohmic contacts on the surfaces of the samples. The results presented in Table 1 are of samples that were grown using temperatures over 800°C, this due to the high

Table 1: Electric measurements obtained by Hall Effect of $Al_xGa_{1-x}As$ layers grown by solid-arsenic-based MOCVD. The table contains the thermodynamic parameters.

Sample	T_m (ºC)	T_{As} (ºC)	n300 (cm^{-3})	n_{77} (cm^{-3})	μ_{300} ($cm^2/V\times s$)	μ_{77} ($cm^2/V\times s$)
57	870	570	1.7×10^{16}	----	2290	----
1173	850	570	4.2×10^{17}	3.9×10^{17}	1272	1173
1235	800	570	2.2×10^{17}	2.3×10^{17}	943	1265

resistivity presented by the samples that were grown below this temperature. The resistivity of the samples obtained with substrate temperatures below of 800°C, in most of cases, made impossible to obtain ohmic contacts for its assessment using the Hall Effect, as has been pointed out. In refs.[6,7] are presented samples grown with solid arsenic in both MOCVD and MBE system, the comparison with the samples presented in this work shows that when the growth temperature is decreased the compensation of samples is increased.

3.5. 12K Photoluminescence measurements of $Al_xGa_{1-x}As$

Figure 3 shows photoluminescence spectrum of the $Al_xGa_{1-x}As$ layer grown at 850°C. As a result of photoluminescence measurements, it could be observed that, the samples grown below 800°C as substrate temperature did not display appreciable signal. In order to obtain photoluminescence signal was necessary to grow the samples using temperatures above 800°C. These temperatures can be considered high in comparison with the temperatures required in other growth systems as is the case of the traditional arsine-MOCVD system[7,8]. Additionally, the temperatures used for growth of the samples studied in this work are not recommended for the case of traditional MOCVD growth system, due to the homogeneous nucleation of the reactants especially for arsine. The weaknesses of the luminescence signal for samples grown at low temperatures, and in some cases the lack of the photoluminescence signal, can be associated with the residual impurities incorporation from the metalorganic precursors. It is widely accepted that oxygen, as a residual impurity, introduces deep traps into $Al_xGa_{1-x}As$ reducing the radiative recombination efficiency[9]. The three dominating non-radiative deep centres, located at about 0.3, 0.5 and 0.8 eV below the conduction band, critically reduce the luminescence efficiency. In Figure 3 is showed a typical photoluminescence spectrum displayed by our grown samples. A common characteristic of these PL spectra is the large linewidth at half-maximum (FWHM) of the peak corresponding to the $Al_xGa_{1-x}As$ excitonic band and the acceptor band. These two bands are contained in a single broad peak with a maximum value situated at 772 nm.

Typical values of the FWHM of our samples were around 70 meV, these values can be considered too large in comparison to the reported in the literature[10]. The FWHM

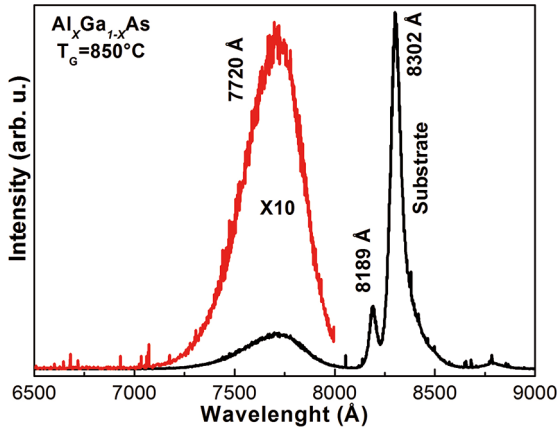

Figure 3: Typical photoluminescence spectrum for MOCVD-$Al_xGa_{1-x}As$ layer, which was grown using metallic arsenic as arsenic precursor.

and shape of this peak make difficult the identification of the $Al_xGa_{1-x}As$ excitonic band to corroborate the aluminium molar concentration that was estimated from the positions of the Raman peaks. In this case we associate this value, with the large incorporation of residual impurities mainly carbon and possibly to the variation of aluminium molar concentration due to mass flow controllers fluctuations. Although, in ref.[11] are presented samples intentionally doped with carbon than display photoluminescence peaks with a FWHM like presented in this work. Additionally, the peaks at 818, 830 and 879 nm can be identified as due to the GaAs substrate and buffer layer emissions.

3.6. $Al_xGa_{1-x}As$ Raman characterization

Figure 4 shows a typical Raman spectrum of the $Al_xGa_{1-x}As$ samples grown with solid arsenic, the growth temperature for this sample was 850°C. In this Raman spectrum can be appreciated that are present five vibrational bands, centred at 275, 377, 555, 654 and 754 cm^{-1}. The bands that have been labelled by a, b, c, d and e can be associated to the GaAs, and AlAs vibrational modes. A standard fitting procedure performed in the interval of 215–445 cm^{-1} suggests this association. Such bands can be deconvoluted in four Lorentzian line shape signals as is shown in figure, which are located at 262, 275, 369, and 377 cm^{-1}. Taking into account that phonons are active in the first-order Raman process in backscattering on the

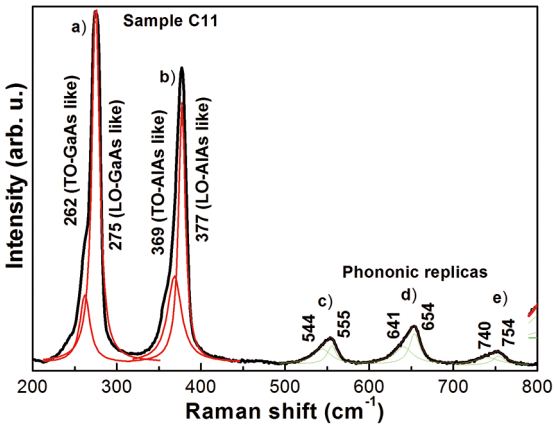

Figure 4: Typical Raman spectrum of $Al_xGa_{1-x}As$ layers that were grown using metallic arsenic as precursor of arsenic.

(001) face, one may assign our vibrational bands to the TO-GaAs-like (262 cm^{-1}), LO-GaAs-like (275 cm^{-1}), TO-AlAs-like (369 cm^{-1}) and LO-AlAs-like (377 cm^{-1}). The low frequency asymmetry of the GaAs-like mode is due to the contribution of the scattering process of phonons with nonzero q vectors that become active due to the alloying disorder process. The TO-GaAs mode, which is forbidden for the (100) orientation of the substrate, becomes active by the breakdown of the selection rules in the backscattering configuration. This breakdown is attributed to structural defects in the alloy; its appearance indicates that the crystal quality of the $Al_xGa_{1-x}As$ layers is not perfect. The modes TO-AlAs like and LO-AlAs like, respectively, are originated on the ternary alloy. The Al composition for the $Al_xGa_{1-x}As$ samples can be determined using the fitted curves that relate the LO-phonon frequency with the aluminium content[8]. In the Raman spectrum (a) the TO and LO GaAs modes at 268 and 292 cm^{-1}, respectively, are clearly distinguishable. In the spectrum (b), the signals at 283.4, 363.2 and 378.7 cm^{-1} assigned to the modes LO-GaAs like, TO-AlAs like and LO-AlAs like, respectively, are originated on the ternary alloy. Due to the thickness of the $Al_xGa_{1-x}As$ epilayers, the modes corresponding to GaAs should not be assigned to the buffer layer. A possible explanation of the presence of the GaAs-like signals is the possible existence of crystalline defects in the epitaxial layers. The forbidden signals are more clearly observed for samples grown at the extreme growth conditions. The Al composition for the $Al_xGa_{1-x}As$ samples can be determined using the fitted curves that relate the LO-phonon frequency with the aluminium content in the $Al_xGa_{1-x}As$ system, according to the next equations[12]:

$$w_{LO}^{GaAs}(x) = 292.2 - 36.7x \ cm^{-1} \quad (1)$$

$$w_{LO}^{AlAs}(x) = 364.7 + 46.7x - 9.4x^2 \ cm^{-1} \quad (2)$$

We can find the Al composition of the ternary films. For the same spectrum (a) and according to the LO-GaAs like and LO-AlAs like peak positions we found x~0.19, the other aluminium molar fractions are shown in Figure 5. As was mentioned before, the spectrum corresponding to a GaAs epilayer, only the LO and TO modes for GaAs are visible. From the same figure, it can be observed that the other vibrational peaks labelled by c, d and e, which are associated with 2LO-GaAs-like, LO-(GaAs+AlAs)-like and 2LO-AlAs-like. In order to determine the behaviour of the Raman spectra with temperature, samples with different growth temperatures were measured and theirs Raman spectra were compared, as is shown in Figure 5. In this figure can be observed the main peaks corresponding to the LO-GaAs and the LO-AlAs, by other side, the TO-GaAs and the TO-AlAs peaks also appear, which as we have pointed out, these modes are forbidden for the configuration used in the measuring of these samples. The presence of these modes are associated with crystalline defects. From the Raman spectra presented in Figure 5 we can conclude, that the crystalline quality of samples is improved when the growth temperature is increased; however, there is a limit beyond which the crystalline quality deteriorates. The forbidden signals are more clearly observed for samples grown at extreme temperature growth conditions. In contrast to what happens with the photoluminescence signal, when the sample growth temperature is increased, the photoluminescence signal intensity increased too, which is indicative of the sample improvement related with the diminishing of deep non radiative recombination centres[13].

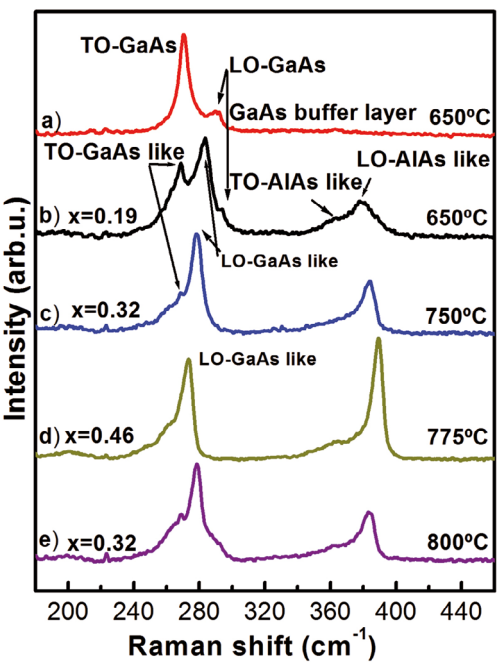

Figure 5: Raman spectra of $Al_xGa_{1-x}As$ epilayers grown at several temperatures by MOCVD using metallic arsenic as precursor. The Al composition values were calculated using the Eqs. (1) and (2), whose values are x~0.19 (b), x~0.32 (c), x~0.46 (c) and x~0.46 (d).

3.7. Surface Morphology

$Al_xGa_{1-x}As$ samples were grown with a wide interval of aluminium molar concentration. In most of the cases the epitaxial layers obtained with growth temperatures below 800°C, presented a hazy surface. In Figure 6 can be observed the typical appearance of samples with an aluminium molar concentration (x) equals to 1 (AlAs).

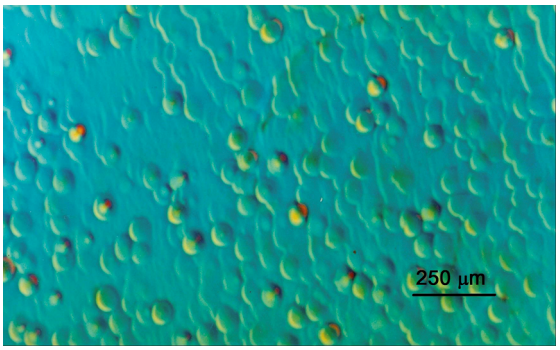

Figure 6: AlAs typical surface.

By other side, the presence of Ga even in small concentration (x not equal to 1) in the AlAs layers to form $Al_xGa_{1-x}As$ layers drastically alter the appearance of the surface, as can be appreciated comparing the pictures presented in Figures 6 and 7. The molar concentration for the layer presented in Figure 7 is x=0.3. In these samples is common to observe a large quantities of oval defects.

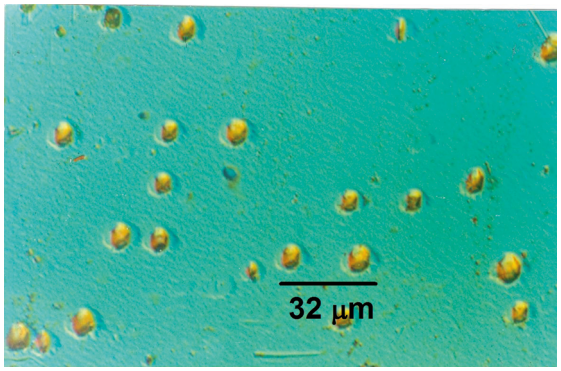

Figure 7: A typical $Al_xGa_{1-x}As$ surface, x=0.3.

3.8. Atomic Force Microscopy (AFM)

For more accurate measurements of the surface roughness, atomic force microscopy scan was carried out. At naked eye, the sample showed in Figure 7 presents a mirror like surface, but as can be appreciated, by means of the atomic force microscopy (AFM) image; the surface presents a high degree of roughness. In this AFM image, the maximum value in the vertical scale is 60 nm as is shown in Figure 8.

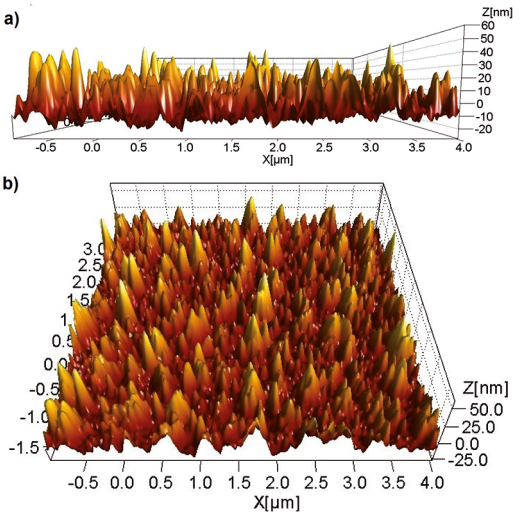

Figure 8: A typical surface of $Al_xGa_{1-x}As$, scanning by AFM, x=0.3.

In comparison with the roughness presented by the GaAs surface in Figure 1, in the case of surface morphology of the ternary alloy illustrated in Figure 8. The increase in the roughness degree can be associated with the impurity incorporation due to the affinity presented by the aluminium and arsenic, mainly with oxygen. This impurity incorporation produces the lattice distortion and stress in the superficial sites, producing the preferential growth in this sites incrementing the roughness. The roughness degree presented by the $Al_xGa_{1-x}As$ represents a serious problem when the goal is the growth of low dimensional structures.

The way in that the heights are distributed on the layer surface can be appreciated in the graph presented in Figure 9. This histogram has been obtained from 100 points over the surface. The more common explanation for the high degree of roughness in these $Al_xGa_{1-x}As$ layers is the low surface mobility of aluminium and arsenic species during the growth process. Furthermore, in our growth system in which AsH_3 has been replaced by elemental arsenic the growth kinetic has been modified due to the fact that the sublimation of metallic arsenic gives As_4 as dominant specie, which have a different surface mobility compared with the mono-atomic As_1 produced by the arsine in traditional MOCVD growth systems. Besides, in traditional systems the arsine decomposition produces ionized hydrogen that promotes a better removal of some impurities as carbon. Additionally, as has been pointed out, the high resistivity of samples grown using low temperatures (<800°C), the weakness of photoluminescence and in some cases the lack of any photoluminescence signal are indicative of large residual impurity incorporation[14].

3.9. $Al_xGa_{1-x}As$ SIMS studies

Although solid arsenic is much less hazardous than AsH_3, there is a price to pay, for the arsine substitution.

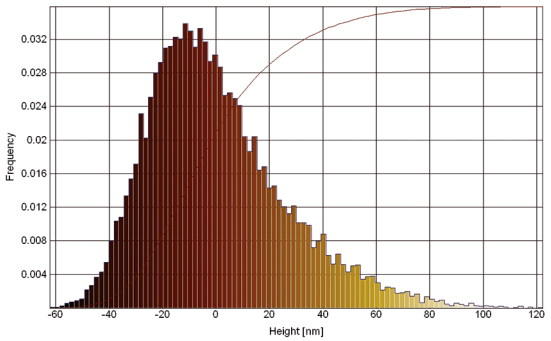

Figure 9: Height distribution histogram.

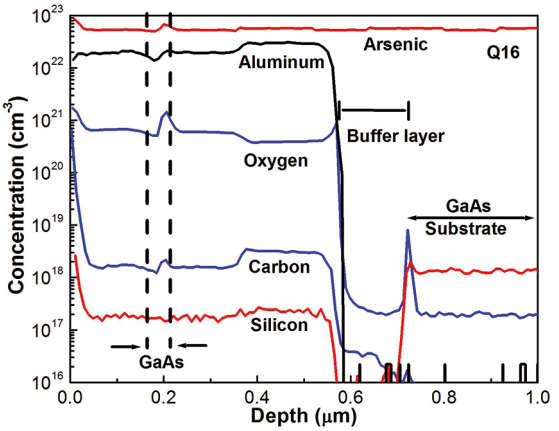

Figure 10: Residual impurity concentration profiles of a typical sample measured by SIMS. Variations of aluminium concentration in the film during growth did not result in increasing oxygen concentration.

The replacement of arsine by solid arsenic will diminish the amount of atomic $As_{1,}$ on the growth surface, and increases the amount of As_4 that is the dominant species produced by the arsenic sublimation this allows the incorporation of impurities as carbon, oxygen, which have a very important deleterious effect on the electrical and optical properties[15]. In Figure 10 can be observe the SIMS composition profile for the sample Q18. This sample was obtained at 850°C as growth temperature, the optical assessment of this sample showed appreciable photoluminescence signal. In the SIMS profile, it can be observed, that for this sample, the oxygen level detected is high although, it must be take into account that the background level in the measurement chamber is high too, as can be seen in the corresponding curve in Figure 10. As in the case of oxygen, the concentration of carbon is very difficult to assess due to the effect of the background levels of these impurities in the analysis chamber. Although, the amount of measured carbon does not correspond exactly to the real concentration in the sample, there is no doubt that the carbon incorporation is important. The carbon incorporation in our samples is caused by the kinetics of decomposition on the growth surface during the sample growth and by the chemical decomposition of the precursors compounds, both the trimethylgallium (TMGa) and trimethyaluminium (TMAl) are compounds consisting of carbon. This carbon is introduced by TMGa pyrolysis, which releases methyl radicals on the growth surface. In the traditional MOCVD, the AsH_3 dissociation on the surface produces hydrogen species, which diffuses and recombines with methyl radicals to produce the stable and volatile methane (CH_4) as byproduct[9]. The hydrogen flux introduced as growth atmosphere does not have significant roll in the surface growth processes due to this hydrogen is not ionized. Another important impurity, detected in our samples is silicon. The importance of this impurity is in the study of the conductivity of the layers. This impurity is a donor impurity in the $Al_xGa_{1-x}As$/GaAs grown by MOCVD, while the carbon has an amphoteric behaviour. In the MOCVD systems, the carbon plays the acceptor roll.

4. Conclusions

In this work, we are reporting the successful growth of $Al_xGa_{1-x}As$ epitaxial layers using a modified MOCVD system and solid arsenic as precursor of V group element. Our samples displayed photoluminescence signal for growth temperatures above 800°C, which is indicative of large incorporation of residual impurities causing the introduction of non-radiative recombination centres. A wide range of growth temperatures were explored but our samples, in general, showed high roughness, this can be considered a serious handicap for the multilayers and quantum well based devices fabrication. We associated these characteristics with the processes of decomposition, diffusion, elimination of byproducts on the growth surface and in general to the modified growth kinetics, by the use of solid arsenic instead arsine. Finally, by SIMS was determined incorporated concentration in the layers, which were mainly oxygen, carbon and silicon.

5. References

1. Peña-Sierra R, Castro-Zavala JG, Escobosa A. Growth of GaAs by MOCVD using a solid arsenic source. *Journal of Crystal Growth*. 1991;107(1-4):337-341.

2. Guillén-Cervantes A, Rivera-Álvarez Z, López-López M, Koudriavtsev I, Sánchez-Reséndiz VM. Photoluminescence and Secondary Ion Mass Spectroscopy characterization of GaAs-AlGaAs quantum wells grown on GaAs (1 0 0) substrates with different surface treatments. *Applied Surface Science*. 2009;255(9):4742-4746.

3. ASTM International. *ASTM F76 - Standard Test Methods for Measuring Resistivity and Hall Coefficient and Determining Hall Mobility in Single-Crystal Semiconductors*. West Conshohocken: ASTM International; 2000.

4. Brozel MR, Stillman GE. *Properties of Gallium Arsenide*. London: Institution of Engineering and Technology; 1996. ISBN 0-85296-885-X.

5. Schläpfer F, Dietsche W, Reichl C, Faelt S, Wegscheider W. Photoluminescence and the gallium problem for highest-mobility GaAs/AlGaAs-based 2d electron gases. *Low temperature MBE growth of high quality AlGaAs, Journal of Crystal Growth*. 2016;442:114-120.

6. Feng J, Clement R, Raynor M. Characterization of high-purity arsine and gallium arsenide epilayers grown by MOCVD. *Low temperature MBE growth of high quality AlGaAs, Journal of Crystal Growth*. 2008;310(23):4780-4785.

7. Shiraki Y, Mishima T, Morioka M. Low temperature MBE growth of high quality AlGaAs. *Low temperature MBE growth of high quality AlGaAs, Journal of Crystal Growth*. 1987;81(1-4):164-168.

8. Seredin PV, Glotov AV, Domashevskaya EP, Arsentyev IN, Vinokurov DA, Tarasov IS. Raman investigation of low temperature AlGaAs/GaAs(1 0 0) heterostructures. *Physica B: Condensed Matter*. 2010;405(12):2694-2696.

9. Huang JW, Kuech TF. Multiple deep levels in metalorganic vapor phase epitaxy GaAs grown by controlled oxygen incorporation. *Applied Physics Letters*. 1994;65(5):604-606.

10. Biefeld RM, Chui HC, Hammons BE, Breiland WG, Brennan TM, Jones ED, et al. High purity GaAs and AlGaAs grown using tertiarybutyllarsine, trimethylaluminum, and trimethylgallium. *Journal of Crystal Growth*. 1996;163(3):212-219.

11. Seredin PV, Domashevskaya EP, Arsentyev IN, Vinokurov DA, Stankevich AL. Properties of epitaxial $(Al_XGa_{1-X}As)_{1-Y}Cy$ alloys grown by MOCVD autoepitaxy. *Semiconductors*. 2013;47(1):7-12.

12. Wasilewski ZR, Dion MM, Lockwood DJ, Poole P, Streater RW, SpringThorpe AJ. Composition of AlGaAs. *Journal of Applied Physics*. 1997;81(4):1683-1694.

13. Saher Helmy A, Bryce AC, Ironside CN, Aitchison JS, Marsh JH. Raman spectroscopy for characterizing compositional intermixing in GaAs/AlGaAs heterostructures. *Applied Physics Letters*. 1999;74(26):3978-3980.

14. Méndez-García VH, Shimomura S, Gorbatchev AY, Cruz-Hernández E, Vázquez-Cortés D. Si-doped AlGaAs/GaAs (6 3 1)A heterostrutures grown by MBE as a function of the As-pressure. *Journal of Crystal Growth*. 2015;425:85-88.

15. Naritsuka S, Kobayashi O, Mitsuda K, Nishinaga T. Oxygen incorporation mechanism in AlGaAs layers grown by molecular beam epitaxy. *Journal of Crystal Growth*. 2003;254(3-4):310-315.